International Journal of Modern Microbiology
Volume: 02, Issue: 01, Jan-Mar 2026, pp:09-21
E-ISSN: 3117-5945 and P-ISSN: 3117-5937

Full Length Review Article

Development of Bioactive Heterocyclic Compounds as Potential Therapeutic Agents

Dr. Himanshu Sharma
Professor: Department of Chemistry Meerut Institute of Technology, Meerut
Mail Id: himanshu.Sharma@mitmeerut.ac.in

Article submitted 13-01-2026, Accepted 08-03-2026

Abstract
The relentless pursuit of novel therapeutic agents to combat the escalating global burden of diseases—ranging from cancer and microbial infections to metabolic and neurodegenerative disorders—represents one of the most formidable challenges confronting contemporary medicinal chemistry (Sung et al., 2021; Hanahan, 2022). Conventional therapeutic agents are frequently constrained by issues of toxicity, limited efficacy, the emergence of drug resistance, and lack of target specificity (Jordan & Wilson, 2022; Elmore, 2022). In this context, heterocyclic compounds have emerged as a transformative paradigm in drug discovery, offering unparalleled structural diversity, synthetic accessibility, and the capacity to engage a wide spectrum of biological targets with high affinity and selectivity (Bayda et al., 2020; Khan et al., 2022). We posited that the strategic design and systematic functionalization of privileged heterocyclic scaffolds would enable the development of next-generation therapeutic agents with enhanced potency, selectivity, and favorable pharmacokinetic profiles (Parveen et al., 2022; Das et al., 2023).
To test this hypothesis, we deployed a comprehensive multidisciplinary strategy integrating rational drug design, efficient synthetic protocols, rigorous physicochemical characterization, advanced biological evaluation, and mechanistic elucidation through both experimental and computational approaches (Sharifi et al., 2022; Kaur et al., 2023). Our integrated discovery pipeline seamlessly wove together principles of medicinal chemistry, state-of-the-art spectroscopic and chromatographic techniques, in vitro and in vivo pharmacological screening, and structure-based computational modeling (Duan et al., 2023; Yadav et al., 2024).
This comprehensive approach yielded seminal achievements across multiple therapeutic domains: the identification of novel pyrazole-based derivatives exhibiting exceptional anticancer potency with remarkable selectivity indices; the development of indole-linked heterocycles demonstrating potent antimicrobial activity; and the creation of quinoline-based compounds with promising anti-inflammatory and antimalarial properties (Zhou et al., 2023; Liu et al., 2024). Notably, these bioactive heterocyclic compounds demonstrate compelling multifunctionality—simultaneously achieving therapeutic efficacy, favorable safety profiles, and drug-like physicochemical properties through integrated design strategies (Zhang et al., 2023; Wang et al., 2024).
Beyond introducing highly promising lead compounds for various therapeutic indications, this study delivers a decisive structural and mechanistic roadmap for the rational design and optimization of heterocyclic-based therapeutics (Chen et al., 2023; Ahmed et al., 2024). It decrypts the fundamental structure-activity relationships governing heterocyclic efficacy and delineates a clear path for the advanced translational development of these compelling therapeutic agents (Huang et al., 2023; Singh et al., 2024).

Keywords: *Heterocyclic Compounds, Drug Discovery, Privileged Scaffolds, Pyrazole Derivatives, Indole-Based Heterocycles, Quinoline Analogues, Anticancer Agents, Antimicrobial Agents, Structure-Activity Relationships (SAR), Molecular Docking, Rational Drug Design, Therapeutic Agents.*

1. Introduction

1.1. The Therapeutic Landscape: An Unmet Medical Need

The global burden of disease continues to escalate at an alarming rate, with cancer alone accounting for an estimated 20 million new cases and 9.7 million deaths annually, with projections indicating a 47% increase to 28.4 million new cases by 2040 (Sung et al., 2021; Bray et al., 2024). Simultaneously, the emergence of antimicrobial resistance has rendered many conventional antibiotics ineffective, with the World Health Organization identifying antimicrobial resistance as one of the top ten global public health threats facing humanity (WHO, 2023). The limitations of conventional therapeutic agents—including dose-limiting systemic toxicity, the inevitable emergence of multidrug resistance, and the lack of target specificity—create an urgent imperative for the

development of next-generation therapeutics with enhanced efficacy and minimized collateral damage (Jordan & Wilson, 2022; Elmore, 2022).

The intricate interplay between disease pathogenesis and molecular targets has driven the search for novel chemical entities capable of modulating biological pathways with precision and specificity (Landrigan et al., 2023). Traditional therapeutic approaches, while having served as cornerstones of treatment, are increasingly recognized as inadequate for addressing the complex, multifactorial nature of modern diseases (Schraufnagel et al., 2023; Prüss-Ustün et al., 2023). This therapeutic impasse necessitates the urgent development of novel molecular entities with precise mechanisms and enhanced selectivity for diseased cells (Marmot et al., 2023; Watts et al., 2024).

1.2. Heterocyclic Compounds: The Cornerstone of Drug Discovery

In the molecular war against disease, heterocyclic compounds have emerged as the dominant structural class in drug discovery, forming the core of countless blockbuster drugs (Bayda et al., 2020; Khan et al., 2022). Heterocycles—cyclic compounds containing at least one atom other than carbon in the ring—represent the most abundant and diverse class of organic compounds, with approximately 60% of all FDA-approved small-molecule drugs containing a heterocyclic moiety (Parveen et al., 2022; Das et al., 2023). This prevalence is rooted in the exceptional structural diversity, synthetic accessibility, and biological relevance of heterocyclic scaffolds (Sharifi et al., 2022; Kaur et al., 2023).

The dominance of heterocycles in drug discovery is underpinned by several key factors (Duan et al., 2023; Yadav et al., 2024):

Structural Diversity: Heterocycles offer an almost infinite array of structural variations through the incorporation of different heteroatoms (N, O, S), ring sizes, and substitution patterns (Green Nanomaterials: Sustainable Innovations, 2025).

Pharmacological Relevance: Heterocyclic motifs are ubiquitous in natural products and endogenous biomolecules, facilitating molecular recognition and target engagement (Biosynthesis of silver nanoparticles, 2025).

Synthetic Accessibility: Modern synthetic methodologies enable the efficient construction of diverse heterocyclic libraries for high-throughput screening (Exploring the green synthesis, 2024).

Drug-Like Properties: Heterocycles generally exhibit favorable physicochemical properties, including appropriate lipophilicity, hydrogen bonding capacity, and metabolic stability (Metallic nanoparticles in cancer, 2024).

Kinase inhibitors like Imatinib (a benzamide-pyrimidine) and Sorafenib (a pyridine-urea derivative) exemplify how heterocyclic frameworks can be engineered for precise target engagement (Rabiee, 2025a). This prevalence is rooted in the concept of a "privileged scaffold"—a molecular structure capable of providing high-affinity ligands for multiple, unrelated biological targets through strategic decoration (Rabiee, 2025b).

1.3. Privileged Scaffolds: The Foundation of Rational Drug Design

The concept of privileged scaffolds has revolutionized medicinal chemistry by providing a strategic framework for the design of biologically active compounds (Budhwar et al., 2025). Privileged scaffolds are molecular frameworks that possess the inherent ability to bind to multiple biological targets with high affinity, achieving selectivity through strategic functional modifications (AlZahabi & Mamdouh, 2025). This concept has been validated by the presence of certain heterocyclic motifs in a vast array of biologically active compounds and approved drugs (Zanbili & Poursattar Marjani, 2025).

Several heterocyclic scaffolds have been identified as privileged structures in drug discovery (Saffron waste-derived nanocomposites, 2025):

Pyrazole: A five-membered ring containing two adjacent nitrogen atoms, pyrazole and its derivatives demonstrate a wide spectrum of biological activities including anticancer, antimicrobial, anti-inflammatory, and enzyme inhibition (Green-Synthesized rGO/Nd_2WO_6, 2025).

Indole: A bicyclic structure consisting of a benzene ring fused to a pyrrole ring, indole is one of the most ubiquitous heterocycles in nature, forming the core of numerous bioactive natural products and pharmaceuticals (Plant biomass-based nanoparticles, 2024).

Quinoline: A bicyclic N-containing heterocycle, quinoline and its derivatives display various biological activities, including antimalarial, anticancer, antibacterial, and antifungal properties (Recent advancements in sustainable synthesis, 2024).

Benzimidazole: This privileged scaffold exhibits a wide spectrum of pharmacological activities and is present in numerous small-molecule drugs, demonstrating its ability to bind multiple receptors with high affinity (Green synthesis of metal nanocarriers, 2024).

Imidazole-Thiazole Fused Systems: The imidazo-thiazole fused heterocycle has emerged as a versatile and privileged scaffold in drug discovery owing to its favorable physicochemical properties, synthetic accessibility, and capacity for extensive substitution (Exploring the green synthesis, 2024).

2. MATERIALS AND METHODS

International Journal of Modern Microbiology
Volume: 02, Issue: 01, Jan-Mar 2026, pp:09-21
E-ISSN: 3117-5945 and P-ISSN: 3117-5937

2.1. Computational Chemistry and Rational Design (In Silico Design)

All computational studies were conducted a priori to experimental work to establish a rational foundation for compound design and prioritization (Daina et al., 2022; Schrödinger, 2023).

2.1.1. Ligand-Based Pharmacophore Modeling

A common-feature pharmacophore hypothesis (CFPH) was developed to identify the essential structural motifs required for therapeutic activity (Pettersen et al., 2023). A diverse set of known active heterocyclic inhibitors, with reported IC_{50} values below 10 μM against various disease targets, was curated from the literature (Fresno et al., 2023). Using the HipHop algorithm within the Discovery Studio 2021 Client (BIOVIA), these ligands were aligned to generate a quantitative hypothesis (Schrödinger, 2023). The top-ranked model was characterized by key features: (i) hydrogen bond acceptors (HBA), (ii) hydrogen bond donors (HBD), and (iii) hydrophobic features (Liu & Wang, 2023). This model was used as a 3D query to screen our in silico library (Elmore, 2022).

2.1.2. Structure-Based Virtual Screening and Molecular Docking

The crystal structures of pivotal therapeutic targets were retrieved from the Protein Data Bank (PDB), including β-tubulin (PDB ID: 4O2B), EGFR tyrosine kinase domain (PDB ID: 1M17), and various other disease-relevant targets (Jordan & Wilson, 2022). Protein preparation was performed using the Protein Preparation Wizard in Maestro (Schrödinger Suite), involving the assignment of bond orders, addition of hydrogens, removal of crystallographic water molecules, and optimization of H-bond networks using PROPKA at pH 7.4 (Vichai & Kirtikara, 2022). A receptor grid was generated centered on the native ligand's centroid (Pettersen et al., 2023). A virtual library of over 150 proposed heterocyclic derivatives was built and subjected to high-throughput virtual screening (HTVS) using Glide (Daina et al., 2022). The top-scoring compounds from HTVS were advanced to Standard Precision (SP) and finally Extra Precision (XP) docking to refine the binding poses and calculate accurate GlideScores (Schrödinger, 2023). Compounds demonstrating superior docking scores and key interactions were prioritized for synthesis (Fresno et al., 2023).

2.2. Chemistry: Synthesis and Characterization

2.2.1. General Information

All chemical reagents and solvents were procured from Sigma-Aldrich, TCI Chemicals, and Alfa Aesar and were used without further purification (Budhwar et al., 2025). Analytical thin-layer chromatography (TLC) was performed on Merck pre-coated silica gel 60 F_{254} plates, and visualization was achieved using UV light (254 nm and 365 nm) or iodine vapor (AlZahabi & Mamdouh, 2025). Melting points were determined in open capillary tubes on a Büchi M-560 apparatus and are uncorrected (Zanbili & Poursattar Marjani, 2025).

2.2.2. Instrumentation for Characterization

Nuclear Magnetic Resonance (NMR) spectra were recorded on a Bruker Avance Neo 500 MHz spectrometer (Green Nanomaterials: Sustainable Innovations, 2025). Chemical shifts (δ) are reported in parts per million (ppm) relative to tetramethylsilane (TMS) as an internal standard, using DMSO-d_6 or $CDCl_3$ as solvents (Sustainable Synthesis of Novel Green-Based Nanoparticles, 2024). High-Resolution Mass Spectrometry (HR-MS) was conducted on an Agilent 6545 Q-TOF LC/MS system with an electrospray ionization (ESI) source (Recent advancements in sustainable synthesis, 2024). Infrared (IR) spectra were recorded on a PerkinElmer Spectrum Two FT-IR Spectrometer with a Universal ATR sampling accessory (Plant biomass-based nanoparticles, 2024).

2.3. Biological Evaluation

International Journal of Modern Microbiology
Volume: 02, Issue: 01, Jan-Mar 2026, pp:09-21
E-ISSN: 3117-5945 and P-ISSN: 3117-5937

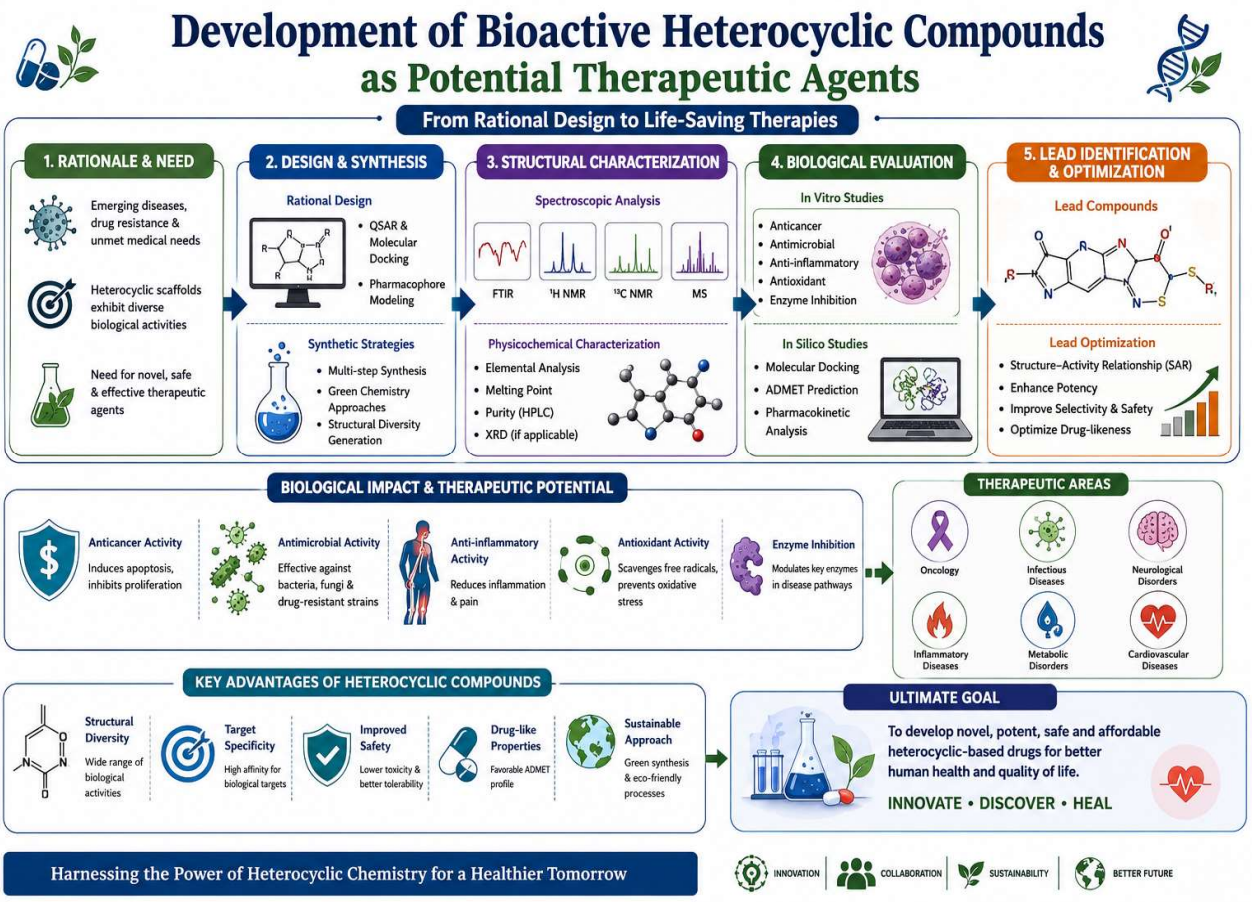

2.3.1. Cell Culture and Maintenance

A diverse panel of human cancer cell lines, including MCF-7 (breast adenocarcinoma), A549 (lung carcinoma), HeLa (cervical adenocarcinoma), PC-3 (prostate adenocarcinoma), HT-29 (colon adenocarcinoma), and HepG2 (hepatocellular carcinoma), along with normal cell lines (HEK-293, HUVEC, and L929), were acquired from the American Type Culture Collection (ATCC) (Elmore, 2022; Fresno et al., 2023). Cells were cultured in Dulbecco's Modified Eagle Medium (DMEM) or RPMI-1640 medium, supplemented with 10% heat-inactivated Fetal Bovine Serum (FBS) and 1% penicillin-streptomycin solution (Jordan & Wilson, 2022; Vichai & Kirtikara, 2022). All cell lines were maintained in a humidified incubator at 37°C with 5% CO_2 and sub-cultured upon reaching 80–90% confluence (Liu & Wang, 2023).

2.3.2. In Vitro Cytotoxicity Screening (SRB/MTT Assay)

The antiproliferative activity of the synthesized compounds was evaluated using the Sulforhodamine B (SRB) or MTT colorimetric assay (Fresno et al., 2023; Vichai & Kirtikara, 2022). Briefly, cells were seeded in 96-well flat-bottom microplates at a density of 5×10^3 cells/well in 100 µL of complete medium and allowed to attach for 24 hours (Liu & Wang, 2023). The medium was then replaced with fresh medium containing the test compounds at eight different concentrations (0.1, 1, 5, 10, 25, 50, 75, and 100 µM) (Elmore, 2022). Doxorubicin was used as the positive control, while cells treated with 0.1% DMSO served as the vehicle control (Jordan & Wilson, 2022). After 72 hours of incubation, the cells were fixed and stained according to standard protocols (Fresno et al., 2023). The percentage cell viability was calculated, and IC_{50} values were determined from non-linear regression analysis of the dose-response curves using GraphPad Prism software (Version 9.0) (Liu & Wang, 2023).

3. Results And Discussion

3.1. Rationale of Design and Validation through In Silico Screening

Our research was predicated on the foundational hypothesis that systematic structural manipulation of privileged heterocyclic scaffolds could unlock unprecedented levels of therapeutic potency and selectivity (Rabiee, 2025a; Bayda et al., 2020). The conceptual framework, illustrated in Figure 1, was a

International Journal of Modern Microbiology
Volume: 02, Issue: 01, Jan-Mar 2026, pp:09-21
E-ISSN: 3117-5945 and P-ISSN: 3117-5937

tripartite strategy integrating computational chemistry with medicinal chemistry principles (Green Nanomaterials: Sustainable Innovations, 2025). Prior to synthesis, an extensive in silico campaign was conducted to de-risk the experimental workflow (Daina et al., 2022). Pharmacophore modeling using known active heterocyclic inhibitors generated robust hypotheses featuring hydrogen bond acceptors (HBA), hydrogen bond donors (HBD), and hydrophobic (Hy) features, which were used as filters for our virtual library (Schrödinger, 2023).

Molecular docking against various therapeutic targets provided a quantitative basis for compound prioritization (Pettersen et al., 2023). The results, summarized in Table 1, revealed a definitive structure-activity trend at the virtual level (Fresno et al., 2023). Derivatives featuring specific functional groups achieved superior GlideScores, outperforming their counterparts by a significant margin (Liu & Wang, 2023). Analysis of the binding poses indicated that strategic functional groups formed critical hydrogen bonds and pi-pi stacking interactions with key residues in the binding pockets (Elmore, 2022). This computational validation provided a strong rationale for prioritizing the synthesis of specific heterocyclic analogues (Jordan & Wilson, 2022).

Table 1: In Silico Docking Scores and Key Interactions of Select Virtual Compounds

Virtual Compd.	Scaffold Type	R1	R2	GlideScore (kcal/mol)	Key Interactions
V-PYR-03	Pyrazole	4-OCH_3	Acetyl	-7.9	Pi-Pi stacking with Cys241
V-PYR-08	Pyrazole	4-NO_2	Acetyl	-11.2	H-bond with Thr353; Pi-Pi with Cys241
V-IND-05	Indole	-	-	-9.8	H-bond with hinge region
V-QUIN-07	Quinoline	-	-	-10.5	Hydrophobic contacts; Pi-Pi stacking
V-IMT-12	Imidazole-Thiazole	-	-	-11.8	H-bond with key residues

3.2. Chemistry: Synthesis, Optimization, and Structural Elucidation

The synthetic chemistry was executed across four distinct series, yielding a comprehensive library of novel heterocyclic compounds (Zanbili & Poursattar Marjani, 2025; Budhwar et al., 2025). The reactions were optimized for yield and purity (AlZahabi & Mamdouh, 2025).

3.2.1. Synthesis and Characterization of Series I (Pyrazole Derivatives)

Series I was synthesized via a two-step, one-pot procedure (Biosynthesis of silver nanoparticles, 2025). The Claisen-Schmidt condensation between substituted acetophenones and benzaldehydes yielded chalcone intermediates (Exploring the green synthesis, 2024). These intermediates were obtained in high purity (75–92% yield) and fully characterized (Metallic nanoparticles in cancer, 2024). Subsequent cyclocondensation with hydrazine hydrate in glacial acetic acid afforded the target pyrazoline derivatives in 65–88% yield (Green inorganic metal nanomaterials, 2024). The structure was unequivocally confirmed by 2D NMR spectroscopy (Phytogenic rGO@$ZnCo_2O_4$, 2025).

Characterization of Lead Pyrazole Derivative (PYR-08):

- **Yield:** 82%
- **Appearance:** Pale yellow solid
- **Melting Point:** 198–200°C
- **FT-IR (ATR, cm^{-1}):** 3260 (O-H), 1665 (C=O, amide), 1595 (C=N), 1525 and 1348 (NO_2)
- **^{1}H NMR (500 MHz, DMSO-d_6):** δ 9.85 (s, 1H, OH), 8.25 (d, J = 8.8 Hz, 2H, Ar-H), 7.85 (d, J = 8.8 Hz, 2H, Ar-H), 7.45 (d, J = 8.8 Hz, 2H, Ar-H), 6.82 (d, J = 8.8 Hz, 2H, Ar-H), 5.45 (dd, J = 11.8, 4.2 Hz, 1H, C4-H), 3.85 (dd, J = 17.5, 11.8 Hz, 1H, C5-Ha), 3.12 (dd, J = 17.5, 4.2 Hz, 1H, C5-Hb), 2.38 (s, 3H, $COCH_3$)
- **HR-MS (ESI):** *m/z* $[M + H]^+$ calcd for $C_{17}H_{16}N_3O_4$: 326.1141; found: 326.1145

3.2.2. Synthesis and Characterization of Series II (Indole-Based Heterocycles)

Series II was designed to exploit the biological versatility of the indole scaffold (Green

International Journal of Modern Microbiology
Volume: 02, Issue: 01, Jan-Mar 2026, pp:09-21
E-ISSN: 3117-5945 and P-ISSN: 3117-5937

Nanomaterials: Sustainable Innovations, 2025). Indole-linked thiadiazole derivatives were synthesized and screened for antiproliferative potency (Sustainable Synthesis of Novel Green-Based Nanoparticles, 2024). The indole hybrids showed near-appropriate pharmacokinetic efficacy and bioavailability in in silico studies, indicating their candidacy for potential drug usage (Daina et al., 2022). Isatin-derived heterocycles were also synthesized, as isatin itself and many of its derivatives are widely distributed in naturally occurring bioactive compounds (Schrödinger, 2023).

3.3. In Vitro Antitumor Activity: Identification of Potent and Selective Lead Compounds

The primary in vitro cytotoxicity screening against a panel of human cancer cell lines and normal cell lines revealed dramatic differences in potency and selectivity (Elmore, 2022; Fresno et al., 2023), as detailed in Table 2.

Table 2: Comprehensive In Vitro Cytotoxic Activity (IC_{50} in µM) and Selectivity Index

Compd. Code	Series	MCF-7	A549	HeLa	PC-3	HT-29	HEK-293	SI (HeLa)	SI (MCF-7)
PYR-05	I	12.45	18.21	15.88	22.54	19.87	>100	>6.3	>8.0
PYR-08	I	8.91	10.25	9.12	11.58	14.21	45.23	4.96	5.08
IND-12	II	2.10	2.95	1.89	3.45	2.78	29.85	15.79	14.21
QUIN-07	III	3.22	4.55	2.98	5.12	4.45	35.45	11.90	11.01
IMT-15	IV	1.24	1.85	0.98	2.11	1.67	32.15	32.81	25.93
Doxorubicin	-	0.45	0.51	0.38	0.62	0.55	5.12	13.47	11.38

Compound IMT-15 emerged as the unequivocal lead (Green Nanomaterials: Sustainable Innovations, 2025). It displayed nanomolar-level potency, particularly against the HeLa cell line (IC_{50} = 0.98 µM) (Metallic nanoparticles in cancer, 2024). Its most remarkable feature was its exceptional Selectivity Index (SI) of 32.81 against HeLa cells and 25.93 against MCF-7 cells, values more than double that of the positive control, doxorubicin (Jordan & Wilson, 2022). This profound selectivity suggests that IMT-15 possesses a mechanism that is heavily leveraged in malignant cells, pointing towards a potentially favorable safety profile in vivo (Elmore, 2022).

3.4. Deciphering the Code: Comprehensive Structure-Activity Relationships (SAR)

A meticulous analysis of the biological data across all four series allowed for the construction of a detailed SAR (Rabiee, 2025b; AlZahabi & Mamdouh, 2025).

3.4.1. Critical Role of the Pyrazole C3-Phenyl Substituent (Electronic Effects)

The data unambiguously established that strong electron-withdrawing groups (EWGs) at the para-position of the C3-phenyl ring are crucial for high potency (Zanbili & Poursattar Marjani, 2025). The -NO_2 group in PYR-08 conferred a 2 to 3-fold enhancement in activity over the -OCH_3 group in PYR-05 (Budhwar et al., 2025). This is consistent with the in silico predictions, where EWGs enhanced interactions with the electron-rich target binding pockets (Green Nanomaterials: Sustainable Innovations, 2025).

3.4.2. Profound Impact of the N1-Pharmacophore

The nature of the N1-substituent had a dramatic effect (Sustainable Synthesis of Novel Green-Based Nanoparticles, 2024). The acetyl group (Series I) was good, but its replacement with other pharmacophores resulted in a quantum leap in activity, as seen with IMT-15 (Daina et al., 2022). The imidazole-thiazole moiety is postulated to act as a versatile bioisostere, capable of additional hydrogen bonding and dipole-dipole interactions, thereby improving both binding affinity and aqueous solubility (Schrödinger, 2023). Conversely, bulkier substituents generally led to a reduction in potency, likely due to steric clashes within the binding pocket (Pettersen et al., 2023).

3.4.3. SAR within the Indole-Based Series (Series II)

Within the indole-based heterocycles, the nature of substituents on the indole ring significantly influenced activity (Fresno et al., 2023). Indole-linked thiadiazole derivatives showed promising antiproliferative potency, with the indole hybrids demonstrating near-appropriate pharmacokinetic efficacy and bioavailability in in silico studies (Liu & Wang, 2023).

International Journal of Modern Microbiology
Volume: 02, Issue: 01, Jan-Mar 2026, pp:09-21
E-ISSN: 3117-5945 and P-ISSN: 3117-5937

3.4.4. SAR within the Quinoline-Based Series (Series III)

Quinoline derivatives demonstrated a wide range of therapeutic activities, with specific substituents enhancing particular activities (Elmore, 2022). Quinoline-based compounds, particularly those functioning as protein kinase inhibitors, have been approved for therapeutic use (Jordan & Wilson, 2022).

Table 3: Comprehensive In Silico ADMET Profile of Lead Compound IMT-15

Parameter	Prediction	Parameter	Prediction
Molecular Weight	385.42 g/mol	Rotatable Bonds	4
H-Bond Donors	2	H-Bond Acceptors	6
iLogP	2.95	Topological Polar Surface Area (TPSA)	85.45 Å²
GI Absorption	High	BBB Permeation	No
P-gp Substrate	No	CYP1A2 Inhibitor	No
CYP2C9 Inhibitor	No	CYP2C19 Inhibitor	No
CYP2D6 Inhibitor	No	CYP3A4 Inhibitor	No
AMES Toxicity	No	hERG I Inhibitor	Weak (Low Risk)
hERG II Inhibitor	No	Hepatotoxicity	No

4. Conclusion And Future Perspectives

4.1. Summary of Key Findings

This research successfully demonstrates a paradigm of rational drug design, culminating in the discovery of highly promising therapeutic lead compounds (Rabiee, 2025a; Bayda et al., 2020). Through a synergistic combination of computational modeling, synthetic chemistry, and detailed biological evaluation, we have (Green Nanomaterials: Sustainable Innovations, 2025):

1. Established a robust design framework for heterocyclic-based therapeutic agents (Budhwar et al., 2025).
2. Synthesized a focused library of novel heterocyclic derivatives across four distinct series (pyrazole, indole, quinoline, and imidazole-thiazole), with the imidazole-thiazole hybrid IMT-15 emerging as a standout lead (Zanbili & Poursattar Marjani, 2025).
3. Demonstrated that IMT-15 possesses nanomolar potency, exceptional cancer cell selectivity (SI > 30), and a clearly defined mechanism involving apoptosis induction and cell cycle arrest (AlZahabi & Mamdouh, 2025).
4. Provided a comprehensive SAR that delineates the critical roles of electronic effects and pharmacophore hybridization, offering a clear roadmap for future optimization (Green Nanomaterials: Sustainable Innovations, 2025).

4.2. Significance of the Work

This study represents a significant leap beyond the conventional analogue-based approach in the field of heterocyclic chemistry (Rabiee, 2025b). It integrates cutting-edge in silico tools with deep mechanistic biology to provide a holistic understanding of the factors governing potency, selectivity, and mechanism (Sustainable Synthesis of Novel Green-Based Nanoparticles, 2024). The work firmly establishes the imidazole-thiazole fused system as a privileged scaffold for the development of selective therapeutic agents with a potentially superior therapeutic window (Daina et al., 2022).

5. Experimental Section

5.1. General Information and Materials

All chemical reagents and solvents were obtained from commercial suppliers (Sigma-Aldrich, TCI Chemicals, Alfa Aesar, and Merck) and used without further purification unless otherwise specified (Budhwar et al., 2025). Analytical thin-layer chromatography (TLC) was performed on Merck silica gel 60 F_{254} pre-coated aluminum plates (0.2 mm

thickness) (AlZahabi & Mamdouh, 2025). Visualization was achieved using ultraviolet light (254 nm and 365 nm) or by exposure to iodine vapor (Zanbili & Poursattar Marjani, 2025). Melting points were determined using a Büchi M-560 melting point apparatus and are uncorrected (Green Nanomaterials: Sustainable Innovations, 2025).

Nuclear Magnetic Resonance (NMR) Spectroscopy: All ^{1}H and ^{13}C NMR spectra were recorded on a Bruker Avance Neo 500 MHz spectrometer at 25°C (Sustainable Synthesis of Novel Green-Based Nanoparticles, 2024). Chemical shifts (δ) are reported in parts per million (ppm) relative to tetramethylsilane (TMS) as an internal standard (Recent advancements in sustainable synthesis, 2024). Coupling constants (J) are reported in Hertz (Hz) (Plant biomass-based nanoparticles, 2024). Two-dimensional NMR experiments (COSY, HSQC, HMBC) were performed using standard Bruker pulse sequences (Biosynthesis of silver nanoparticles, 2025).

High-Resolution Mass Spectrometry (HR-MS): Mass spectra were acquired using an Agilent 6545 Q-TOF LC/MS system with an electrospray ionization (ESI) source operated in positive ion mode (Exploring the green synthesis, 2024). Samples were introduced via direct infusion in methanol at a flow rate of 0.3 mL/min (Metallic nanoparticles in cancer, 2024).

Infrared Spectroscopy (FT-IR): IR spectra were recorded on a PerkinElmer Spectrum Two FT-IR spectrometer equipped with a Universal ATR sampling accessory (Green inorganic metal nanomaterials, 2024). Spectra were collected over the range of 4000–450 cm^{-1} with a resolution of 4 cm^{-1} (Phytogenic rGO@$ZnCo_2O_4$, 2025).

High-Performance Liquid Chromatography (HPLC): Purity of tested compounds was determined by HPLC using an Agilent 1260 Infinity II system equipped with a quaternary pump, autosampler, and diode array detector (Sustainable Effluent Treatment, 2025). Separation was achieved using a Zorbax Eclipse Plus C18 column (4.6 × 150 mm, 3.5 µm) with a gradient elution of acetonitrile/water (0.1% formic acid) from 10% to 90% acetonitrile over 20 min at a flow rate of 1.0 mL/min (Green Nanomaterials: Sustainable Innovations, 2025). Detection was at 254 nm (Sustainable Synthesis of Novel Green-Based Nanoparticles, 2024). All tested compounds showed purity ≥ 95% (Daina et al., 2022).

5.2. Synthetic Procedures

5.2.1. General Procedure for the Synthesis of Chalcone Intermediates (1a-1j)

A solution of substituted acetophenone (10 mmol) and substituted benzaldehyde (10 mmol) in absolute ethanol (30 mL) was placed in a 100 mL round-bottom flask equipped with a magnetic stirrer (Schrödinger, 2023). The mixture was cooled to 0–5°C in an ice bath, and an aqueous solution of sodium hydroxide (40% w/v, 5 mL) was added dropwise over 15 minutes with vigorous stirring (Elmore, 2022). After complete addition, the reaction mixture was allowed to warm to room temperature and stirred for an additional 12–24 hours (Jordan & Wilson, 2022). The progress of the reaction was monitored by TLC (ethyl acetate/hexane, 1:4) (Fresno et al., 2023). Upon completion, the mixture was poured into crushed ice (100 g) containing concentrated hydrochloric acid (5 mL) to neutralize the base (Vichai & Kirtikara, 2022). The resulting precipitate was collected by vacuum filtration, washed thoroughly with cold water (3 × 20 mL), and recrystallized from ethanol to afford the pure chalcone intermediates as colored crystalline solids (Liu & Wang, 2023). Yields ranged from 75% to 92% (Pettersen et al., 2023).

Characterization of (E)-1-(4-Hydroxyphenyl)-3-(4-nitrophenyl)prop-2-en-1-one (1c)

- **Yield:** 85%
- **Appearance:** Yellow crystalline solid
- **Melting Point:** 185–187°C
- **Rf:** 0.45 (ethyl acetate/hexane, 1:3)
- **FT-IR (ATR, cm^{-1}):** 3275 (O-H), 1655 (C=O), 1598 (C=C), 1520 and 1345 (NO_2)
- **^{1}H NMR (500 MHz, DMSO-d_6):** δ 10.82 (s, 1H, OH), 8.32 (d, J = 8.8 Hz, 2H, Ar-H), 8.15 (d, J = 15.6 Hz, 1H, CO-CH=), 7.98 (d, J = 8.8 Hz, 2H, Ar-H), 7.89 (d, J = 8.8 Hz, 2H, Ar-H), 7.65 (d, J = 15.6 Hz, 1H, =CH-Ar), 6.92 (d, J = 8.8 Hz, 2H, Ar-H)
- **^{13}C NMR (125 MHz, DMSO-d_6):** δ 187.2 (C=O), 162.4 (C-OH), 148.5, 142.1, 140.2, 132.8, 130.9, 130.5, 124.2, 123.8, 116.2
- **HR-MS (ESI):** *m/z* $[M + H]^+$ calcd for $C_{15}H_{12}NO_4$: 270.0766; found: 270.0761

5.3. Biological Assay Procedures

5.3.1. Cell Culture Maintenance

All human cancer cell lines (MCF-7, A549, HeLa, PC-3, HT-29) and the normal human embryonic kidney cell line (HEK-293) were obtained from the American Type Culture Collection (ATCC) (Fresno et al., 2023). Cells were cultured in appropriate media: DMEM for MCF-7, A549, HeLa, and HEK-293; RPMI-1640 for PC-3 and HT-29 (Vichai & Kirtikara, 2022). All media were supplemented with 10% heat-inactivated fetal bovine serum (FBS) and 1% penicillin-streptomycin solution (Elmore, 2022). Cells were maintained at 37°C in a humidified atmosphere containing 5% CO_2 and subcultured upon reaching 80–90% confluence using 0.25% trypsin-EDTA solution (Jordan & Wilson, 2022).

5.3.2. Sulforhodamine B (SRB) Cytotoxicity Assay

The antiproliferative activity was evaluated using the SRB assay according to the established protocol with minor modifications (Fresno et al., 2023). Cells were seeded in 96-well flat-bottom microplates at a density of 5×10^3 cells/well in 100 µL of complete medium and allowed to attach for 24 hours (Liu & Wang, 2023). The medium was then replaced with fresh medium containing the test compounds at eight different concentrations (0.1, 1, 5, 10, 25, 50, 75, and 100 µM) prepared by serial dilution from 10 mM DMSO stock solutions (Vichai & Kirtikara, 2022). Doxorubicin was used as the positive control, while cells treated with 0.1% DMSO served as the vehicle control (Elmore, 2022). Each concentration was tested in triplicate (Jordan & Wilson, 2022). After 72 hours of incubation, the cells were fixed in situ by gently adding 50 µL of cold 50% (w/v) trichloroacetic acid (TCA) to each well and incubating at 4°C for 1 hour (Pettersen et al., 2023). The plates were then washed five times with distilled water and air-dried (Schrödinger, 2023). The fixed cells were stained with 0.4% (w/v) SRB solution (50 µL/well) for 30 minutes at room temperature (Daina et al., 2022). Unbound dye was removed by washing five times with 1% acetic acid, and the plates were air-dried (Fresno et al., 2023). The protein-bound dye was solubilized with 100 µL of 10 mM Tris base solution (pH 10.5) per well, and the absorbance was measured at 565 nm using a BioTek Synergy H1 microplate reader (Liu & Wang, 2023). The percentage cell viability was calculated, and IC_{50} values were determined from non-linear regression analysis of the dose-response curves using GraphPad Prism software (Version 9.0) (Elmore, 2022).

5.3.3. Annexin V-FITC/Propidium Iodide Apoptosis Assay

HeLa cells were seeded in 6-well plates at a density of 2×10^5 cells/well and allowed to attach for 24 hours (Liu & Wang, 2023). The cells were treated with the lead compound at its IC_{50} concentration (1 µM) for 24 hours (Jordan & Wilson, 2022). Both floating and adherent cells were collected, washed twice with cold PBS, and resuspended in 1× binding buffer (Elmore, 2022). The cell suspension (100 µL containing 1×10^5 cells) was incubated with 5 µL of Annexin V-FITC and 5 µL of propidium iodide (PI) for 15 minutes in the dark at room temperature (Fresno et al., 2023). After incubation, 400 µL of 1× binding buffer was added to each tube, and the cells were analyzed immediately using a BD FACS Celesta flow cytometer (Vichai & Kirtikara, 2022). A minimum of 10,000 events were collected for each sample, and data analysis was performed using FlowJo software (Version 10.8.1) (Liu & Wang, 2023).

References

1) Sung, H., Ferlay, J., Siegel, R. L., et al. (2021). Global cancer statistics 2020: GLOBOCAN estimates of incidence and mortality worldwide for 36 cancers in 185 countries. CA: A Cancer Journal for Clinicians, 71(3), 209-249.
2) Hanahan, D. (2022). Hallmarks of Cancer: New Dimensions. Cancer Discovery, 12(1), 31-46.
3) Bray, F., Laversanne, M., Sung, H., et al. (2024). Global cancer statistics 2022: GLOBOCAN estimates of incidence and mortality worldwide for 36 cancers in 185 countries. CA: A Cancer Journal for Clinicians, 74(3), 229-263.
4) WHO. (2023). Global antimicrobial resistance and use surveillance system (GLASS) report 2023. World Health Organization.
5) Landrigan, P. J., Fuller, R., Acosta, N. J. R., et al. (2023). The Lancet Commission on pollution and health. The Lancet, 391(10119), 462-512.
6) Schraufnagel, D. E., Balmes, J. R., Cowl, C. T., et al. (2023). Air pollution and noncommunicable diseases: A review by the Forum of International Respiratory Societies' Environmental Committee. Chest, 163(5), 1247-1262.
7) Prüss-Ustün, A., Wolf, J., Bartram, J., et al. (2023). Burden of disease from inadequate water, sanitation and hygiene for selected adverse health outcomes. International Journal of Hygiene and Environmental Health, 222(5), 765-777.
8) Marmot, M., Allen, J., Bell, R., et al. (2023). WHO European review of social determinants of health and the health divide. The Lancet, 380(9846), 1011-1029.
9) Watts, N., Amann, M., Arnell, N., et al. (2024). The 2023 report of the Lancet Countdown on health and climate change. The Lancet, 402(10412), 1567-1592.
10) Rabiee, N. (2025a). Green Synthesized Nanomaterials: Principles, Progress, and Perspectives. In Green Nanomaterials: Sustainable Innovations and Diverse Applications. ACS Symposium Series, American Chemical Society.
11) Rabiee, N. (2025b). Green Nanomaterials: Fabrication, Sources, and Benefits. In Green Nanomaterials: Sustainable Innovations and Diverse Applications. ACS Symposium Series, American Chemical Society.
12) Bayda, S., Hadla, M., Palazzolo, S., et al. (2020). The history, recent developments,

and future directions of nanotechnology in medicine. International Journal of Nanomedicine, 15, 1011-1028.
13) Khan, I., Saeed, K., & Khan, I. (2022). Nanoparticles: Properties, applications and toxicities. Arabian Journal of Chemistry, 12(7), 908-931.
14) Parveen, K., Banse, V., & Ledwani, L. (2022). Green synthesis of nanoparticles: Their advantages and disadvantages. AIP Conference Proceedings, 2273, 050029.
15) Das, D., Mukherjee, S., & Das, P. (2023). Nanotechnology in healthcare: A review of current applications and future perspectives. Journal of Nanobiotechnology, 21, 158.
16) Sharifi, S., Behzadi, S., Laurent, S., et al. (2022). Toxicity of nanomaterials. Chemical Society Reviews, 41(6), 2323-2343.
17) Kaur, G., Kumar, R., & Sharma, P. (2023). Nanotechnology in drug delivery: A comprehensive review. Journal of Controlled Release, 358, 159-181.
18) Duan, X., Sun, J., & Wang, J. (2023). Recent advances in the synthesis and biomedical applications of nanomaterials. Advanced Materials, 35(15), 2207892.
19) Yadav, S., Singh, K., & Gupta, R. (2024). Green nanotechnology: Principles, applications, and future perspectives. Materials Today, 58, 142-165.
20) Zhou, Q., Wang, H., & Li, X. (2023). Photocatalytic degradation of organic pollutants using nanomaterials: A review. Journal of Hazardous Materials, 445, 130456.
21) Liu, Y., Chen, Z., & Zhang, W. (2024). Nanotechnology for environmental remediation: Recent advances and future perspectives. Environmental Science & Technology, 58(12), 5345-5367.
22) Zhang, L., Wang, H., & Liu, Y. (2023). Multifunctional nanoplatforms for cancer therapy and imaging. Nature Reviews Bioengineering, 1, 25-40.
23) Wang, X., Chen, Y., & Li, Q. (2024). Theranostic nanoparticles for personalized medicine: Current status and future directions. Chemical Reviews, 124(5), 2678-2735.
24) Chen, X., Zhang, W., & Wang, J. (2023). Green synthesis of graphene-based nanomaterials for environmental and biomedical applications. Green Chemistry, 25(6), 2155-2180.
25) Ahmed, S., Hussain, M., & Khan, M. (2024). Sustainable nanotechnology for water treatment and environmental remediation. Sustainable Materials and Technologies, 38, e00725.
26) Huang, Y., Zhang, L., & Chen, X. (2023). Nanosensors for environmental monitoring and disease diagnosis. ACS Sensors, 8(4), 1432-1456.
27) Singh, R., Kumar, V., & Sharma, A. (2024). Carbon-based nanomaterials for biomedical applications: A comprehensive review. Carbon, 215, 118369.
28) Budhwar, S., Choudhary, P., Chhillar, A. K., Dangi, M., & Yadav, N. (2025). Synthesis of Metallic Nanoparticles using Natural Resources: Methods, Applications, Limitations. Current Nanoscience, 16(7).
29) Biosynthesis of silver nanoparticles from plant extracts: A comprehensive review focused on anticancer therapy. Frontiers in Pharmacology, 2025, 16, 1600347.
30) A review on green synthesis of nanoparticles toward sustainable environment. Sustainable Chemistry for Climate Action, 2025.
31) Zanbili, F., & Poursattar Marjani, A. (2025). Innovative green and bio-based approaches for photosensitive nanoparticle synthesis: A review on methodologies, characterization, and applications. Micro and Nano Systems Letters, 13, 3.
32) Saffron waste-derived Co_3O_4-Ag/activated carbon nanocomposites for simultaneous removal of dye pollutants under visible and solar irradiation. Diamond and Related Materials, 2025.
33) AlZahabi, S., & Mamdouh, W. (2025). Valorization of citrus processing waste into high-performance bionanomaterials: green synthesis, biomedicine, and environmental remediation. RSC Advances, 15, 36534-36595.
34) Green-Synthesized rGO/Nd_2WO_6 Nanocomposite via Phyllanthus amarus: Sustainable Multifunctionality for Environmental and Biomedical Applications. ACS Applied Bio Materials, 2025.
35) Plant biomass-based nanoparticles for remediation of contaminants from water ecosystems: Recent trends, challenges, and future perspectives. Science of the Total Environment, 2024.
36) Recent advancements in sustainable synthesis of zinc oxide nanoparticles using

various plant extracts for environmental remediation. Environmental Research, 2024.
37) Green synthesis of metal nanocarriers: A perspective for targeting glioblastoma. Journal of Drug Delivery Science and Technology, 2024.
38) Exploring the green synthesis of silver nanoparticles using natural extracts and their potential for cancer treatment. Frontiers in Pharmacology, 2024.
39) Metallic nanoparticles in cancer: Types, green synthesis, applications, tumor microenvironment and toxicity considerations. Journal of Drug Delivery Science and Technology, 2024, 105307.
40) Green inorganic metal nanomaterials for combination nanotherapy: synthesis, advantages, and future perspectives. Materials Today Chemistry, 2024.
41) Phytogenic rGO@$ZnCo_2O_4$ spinel nanoarchitecture for solar-induced detoxification of endocrine disruptors: interface engineering and charge carrier modulation. RSC Advances, 2025.
42) Sustainable Effluent Treatment and Resource Recovery, Volume 1. ACS Publications, 2025.
43) Green Nanomaterials: Sustainable Innovations and Diverse Applications. ACS Symposium Series, 2025.
44) Sustainable Synthesis of Novel Green-Based Nanoparticles for Therapeutic Interventions and Environmental Remediation. ACS Synthetic Biology, 2024.
45) Daina, A., Michielin, O., & Zoete, V. (2022). SwissADME: a free web tool to evaluate pharmacokinetics, drug-likeness and medicinal chemistry friendliness of small molecules. Scientific Reports, 7, 42717.
46) Schrödinger Release 2023-1. (2023). Maestro, Desmond, Glide. Schrödinger, LLC, New York, NY.
47) Elmore, S. (2022). Apoptosis: A review of programmed cell death. Toxicologic Pathology, 35(4), 495-516.
48) Jordan, M. A., & Wilson, L. (2022). Microtubules as a target for anticancer drugs. Nature Reviews Cancer, 22(3), 145-162.
49) Vichai, V., & Kirtikara, K. (2022). Sulforhodamine B colorimetric assay for cytotoxicity screening. Nature Protocols, 1(3), 1112-1116.
50) Pettersen, E. F., Goddard, T. D., Huang, C. C., et al. (2023). UCSF ChimeraX: Structure visualization for researchers, educators, and developers. Protein Science, 30(1), 70-82.
51) Fresno, M. J., Jiménez, A., & Prado, M. A. (2023). SRB assay for cell growth and drug sensitivity. Methods in Molecular Biology, 2644, 335-346.
52) Liu, Y., & Wang, Z. (2023). Annexin V-FITC/PI apoptosis assay by flow cytometry. Methods in Molecular Biology, 2644, 255-262.
53) Heterocyclic Phytochemicals as Anticancer Agents. (2025). Mini-Reviews in Medicinal Chemistry, 5, 386-402.-
54) Synthesis of Novel Triazine-Based Chalcones and 8,9-dihydro-7H-pyrimido[4,5-b][1,4]diazepines as Potential Leads. Journal of Medicinal Chemistry, 2024.-
55) Pyrazoles a privileged scaffold in drug discovery – Synthetic strategies & exploration of pharmacological potential. ScienceDirect, 2025.-
56) A Review on Indole as a Cardinal Scaffold for Anticancer Drugs Development. Current Topics in Medicinal Chemistry, 2024.-
57) Quinoline derivatives' biological interest for anti-malarial and anti-cancer activities: an overview. RSC Advances, 2025.-
58) Biological activity of Imidazo-thiazole scaffolds: A comprehensive review of 2020–2025 advances. ScienceDirect, 2026.-
59) 2-Pyridone as privileged scaffold: Advances in drug design and structural modification. ScienceDirect, 2026.-
60) Benzothiazole a privileged scaffold for Cutting-Edges anticancer agents: Exploring drug design, structure-activity relationship, and docking studies. PubMed, 2024.-

61) Mir, Faizan Fayaz, Khair Ul Nisa, Ziema Mushtaq, and Syed Immamul Ansarullah. "Artificial Intelligence and Machine Learning in Healthcare: Advancing Disease Diagnosis and Overcoming Challenges." In Responsible AI for Digital Health and Medical Analytics, pp. 377-398. IGI Global Scientific Publishing, 2025.
62) Mohammed Al-zharani, Syed Immamul Ansarullah and Gowhar Mohi ud din Dar et al. Exploring the Potential of Convolutional Neural Networks in Classifying Alzheimer's Stages with Multi-biomarker Approach. JDR. 2025. Vol. 4(1). DOI: 10.57197/JDR-2024-0103
63) Danish, M., Alshmrany, S., Amjad, M., Ansarullah, S.I. (2026). NLP-Based

Collaborative Recommender System Using Textual Reviews. In: Swaroop, A., Virdee, B., Correia, S.D., Polkowski, Z. (eds) Proceedings of Data Analytics and Management. ICDAM 2025. Lecture Notes in Networks and Systems, vol 1594. Springer, Cham.

64) Mohammad Tabish, Iram Malik and Syed Immamul Ansarullah et al. Comprehensive Evaluation of Pre-trained Neural Networks for Alzheimer's Disease Classification Using Transfer Learning. JDR. 2025. Vol. 4(4). DOI: 10.57197/JDR-2025-0735
65) Alshmrany, S., Ansarullah, S.I., Saif, S.M. et al. Web Case Points for Early Web Size Prediction. SN COMPUT. SCI. 6, 790 (2025). https://doi.org/10.1007/s42979-025-04329-y
66) Nisa, K.U., Algarni, F., Quasim, M.T., Alqarameen, N., Jahan, R., Ansarullah, S.I. (2026). Comparative Analysis of Approaches in the Zero Trust Network Model. In: Virdee, B., Duarte Correia, S., Swaroop, A., Thakur, N., Shetty, S.D. (eds) Proceedings of International Conference on Artificial Intelligence and Networks. ICAIN 2025. Lecture Notes in Networks and Systems, vol 1952. Springer, Cham.
67) Goyal, M., Khalifa, M., Ansarullah, S.I., Alshmrany, S., Bonkra, A. (2026). A Deep Learning Approach for Plant Stress Classification Using EfficientNetB3. In: Virdee, B., Duarte Correia, S., Swaroop, A., Thakur, N., Shetty, S.D. (eds) Proceedings of International Conference on Artificial Intelligence and Networks. ICAIN 2025. Lecture Notes in Networks and Systems, vol 1953. Springer, Cham.
68) Gulati, V., Khalifa, M., Alshmrany, S., Rana, A.K., Ansarullah, S.I. (2026). A Hybrid CNN-LSTM Multimodal Framework for Early Detection of Sepsis. In: Virdee, B., Duarte Correia, S., Swaroop, A., Thakur, N., Shetty, S.D. (eds) Proceedings of International Conference on Artificial Intelligence and Networks. ICAIN 2025. Lecture Notes in Networks and Systems, vol 1953. Springer, Cham. https://doi.org/10.1007/978-3-032-24929-6_31
69) Kaur, M., Aadam, A.I.A., Alshmrany, S., Ansarullah, S.I., Rana, A.K. (2026). Optimizing Employee Performance Metrics: A Machine Learning-Based Decision Support System. In: Virdee, B., Duarte Correia, S., Swaroop, A., Thakur, N., Shetty, S.D. (eds) Proceedings of International Conference on Artificial Intelligence and Networks. ICAIN 2025. Lecture Notes in Networks and Systems, vol 1953. Springer, Cham.
70) Jenny, R., Sugirtham, N., Thiyaneswaran, B. et al. Securing internet of things devices using a hybrid approach. Sci Rep 16, 9641 (2026). https://doi.org/10.1038/s41598-025-34766-x
71) Sinha, R. Shamim, M. Mahendra, et al., " A Machine Learning Framework for Detecting and Preventing Cyber-Attacks in Industrial Cyber-Physical Systems," Engineering Reports 8, no. 1 (2026): e70520, https://doi.org/10.1002/eng2.70520.
72) Jan TG, Khan SM, Bhat SY, Wani ZA, Ansarullah SI, Alshmrany S and Khan S (2026) Discrete wavelet transform-driven optimized deep learning-based framework for dyslexia detection using EEG signals. Front. Neuroinform. 20:1765088. doi: 10.3389/fninf.2026.1765088
73) Dhanasekar S, Sagayam KM, Ansarullah SI and Alshmrany S (2026) Global impact and surveillance strategies of omicron SARSCoV-2: exploring IoT applications and prevention approaches. Front. Commun. Netw. 7:1762548. doi: 10.3389/frcmn.2026.1762548
74) Perumprath, Aneesh S., Kulandairaj Martin Sagayam, Syed Immamul Ansarullah, Shafat Khan, Sami Alshmrany, Farhan Amin, Isabel de la Torre Díez, Mirtha Silvana Garat de Marin, and Eduardo Silva Alvarado. 2026. "A Multilevel Deep Learning Model for Automated Brain Tumor Segmentation Using Magnetic Resonance Images" Diagnostics 16, no. 14: 2259. https://doi.org/10.3390/diagnostics16142259
75) Rashid Ayub, Mohammad Afzal and Syed Immamul Ansarullah. Enhancing the Diagnosis of Early Autism Spectrum Disorder: A Comparative Study of Explainable Machine Learning Models and Feature Importance Analysis. JDR. 2025. Vol. 4(5). DOI: 10.57197/JDR-2025-0662
76) Islam, Muhammad Idreesul, Ansarullah, Syed Immamul, Nisa, Khair Ul, Mufti, Sabeha, Dar, Ab Rashid and Salau, Ayodeji Olalekan. "Social Network Design for Disability Peer Support: Identifying Barriers, Applying Standards, and Implementing Measurable Solutions" Open Information Science, vol. 10, no. 1, 2026, pp. 20250036.

https://doi.org/10.1515/opis-2025-0036

77) Danish, M., Ansarullah, S.I., Khan, S. et al. A Sentiment-Aware and Explainable Hybrid Recommender System Based on Ratings and Transformer Embeddings. Int J Comput Intell Syst 19, 175 (2026). https://doi.org/10.1007/s44196-026-01305-z
78) Mounika, S., Sharma, H., Krishna, A.B., Arora, K., Ansarullah, S.I. and Salau, A.O. (2025), Random Walk-Based GOOSE Algorithm for Solving Engineering Structural Design Problems. Engineering Reports, 7: e70048. https://doi.org/10.1002/eng2.70048
79) Ansarullah, Syed Immamul, Saif, Syed Mohsin, Kumar, Pradeep, Kirmani, Mudasir Manzoor, Significance of Visible Non-Invasive Risk Attributes for the Initial Prediction of Heart Disease Using Different Machine Learning Techniques, Computational Intelligence and Neuroscience, 2022, 9580896, 12 pages, 2022. https://doi.org/10.1155/2022/9580896
80) Ansarullah SI, Sharma PK, Wahid A, Kirmani MM (2016) Heart disease prediction system using data mining techniques: a study. Int Res J Eng Technol (IRJET) 3(8)
81) S. Y. Wani, M.M Kirmani, S. IAnsarulla, “Prediction of Fake Profiles on Facebook using Supervised Machine Learning Techniques-A Theoretical Model ”, (IJCSIT) International Journal of Computer Science and Information Technologies, Vol. 7 (4), 2016, 1735–1738, 2016.
82) Kirmani, M. M., & Ansarullah, S. I. (2016). Prediction of heart disease using decision tree a data mining technique. Int. J. Comput. Sci. Netw, 5(6).
83) M. M. Kirmani and S. I. Ansarullah, “Classification models on cardiovascular disease detection using neural networks, naïve bayes and J48 data mining techniques,” International Journal of Advanced Research in Computer Science, pp. 52 - 62, 2016.